ChemComm

Check for updates

A streamlined steric-shielding approach toward efficient narrowband (FWHM ∼ 18 nm) ultra-violet emitters for OLEDs

Ankit Kumar,†[a] Seungwon Han,†[b] Dilip Kumar Sharma,[a] Jun Yeob Lee [ID] *[bcd] and Rajendra Kumar Konidena [ID] *[a]

Herein, a simple, yet versatile molecular design was unraveled to develop a narrowband ultraviolet (UV) emitter by strategically integrating indolo[3,2,1-*jk*]carbazole and carbazole through a non-conjugative mode. The compound exhibited pure UV emission (λ_{em} ∼ 380 nm) with a narrow FWHM of 18 nm. When utilized as an emitter in OLEDs, it exhibited a maximum EQE of 3.5% and CIEy of 0.037. As a host for a green phosphorescent OLED, it demonstrated an EQE of 22.9% with an impressively low roll-off of 4% at 3000 cd m^{-2}.

Narrowband emissive pure organic emitters have emerged as crucial components in the development of ultra-high-definition organic light-emitting diodes (OLEDs).[1] During the past two decades, tremendous progress has been made in crafting efficient red, green, and blue emitters.[1] More recently, there has been a growing focus on shifting the emission wavelengths of organic materials at either end of the electromagnetic spectrum, unlocking new opportunities for next-generation OLED applications.[2] Of these, ultraviolet (UV) emitters with emission wavelengths ≤400 nm are of particular interest due to their utility as excitation sources for generating primary colors—red, green, and blue—as well as white light. Beyond display technology, UV-emitting materials find relevance in diverse areas such as sterilization, biomedical imaging, photocatalysis, water purification, sensing, and high-density data storage.[3] Traditional donor–acceptor (D–A) fluorophores provide versatile platforms for tailoring electronic and optical properties, supporting emission tunability from the blue to the near-infrared region.[4] However, many D–A structured molecules—especially those exhibiting thermally activated delayed fluorescence (TADF)—tend to display broad emission profiles, often with spectral full-width-at-half-maximum (FWHM) values in the range of 70–100 nm.[4] This spectral broadening arises largely due to conformational relaxation and vibronic interactions associated with the intramolecular charge transfer (ICT) excited states. To overcome this limitation, researchers have turned to rigid, planar polycyclic aromatic hydrocarbons (PAHs), which help suppress geometric reorganization upon excitation.[5] Some PAHs further exploit alternating resonance effects between electron-rich (O, S and N) and electron-deficient B-atoms to spatially separate the highest occupied molecular orbital (HOMO) and lowest unoccupied molecular orbital (LUMO).[5] This configuration gives rise to a multiple-resonance (MR) effect, which enables emitters with exceptionally narrow FWHM < 30 nm. The resulting short-range CT states reduce exchange interactions and facilitate efficient reverse inter-system crossing (RISC), making MR-TADF emitters particularly effective for harvesting triplet excitons. These materials have achieved impressive OLED performance, with remarkable external quantum efficiencies (EQEs). Nonetheless, achieving UV emission (<400 nm) in MR-TADF systems remains a formidable challenge.[6] The rigid resonance framework responsible for narrowband emission typically lacks the tunability needed to reach such short wavelengths. Additionally, they often suffer from complex synthetic procedures, expensive raw materials and low yields, limiting their practical scalability. Nonetheless, simultaneous achievement of UV emission and narrow FWHM < 20 nm without B-PAHs has become a long-standing challenge.

Besides the MR approach, another effective strategy to achieving narrowband emission with high excited-state energy involves the deliberate integration of rigid molecular building blocks. By minimizing interchromophoric interactions and restricting excited-state structural relaxation, such designs can significantly suppress vibronic coupling. Although several UV or near-UV (NUV) emitters incorporating rigid chromophores have been reported, many still suffer from broad emission profiles (FWHM > 30 nm),

[a] Organic Materials Laboratory (OML), Department of Chemistry, Indian Institute of Technology-Patna, Bihta Kanpa Rd, Patna, Dayalpur Daulatpur, Bihar 801106, India. E-mail: rajsan@iitp.ac.in, rkonidena531@gmail.com

[b] Department of Display Convergence Engineering, Sungkyunkwan University 2066, Seobu-ro, Jangan-gu, Suwon, Gyeonggi, 16419, Republic of Korea. E-mail: leej17@skku.edu

[c] School of Chemical Engineering, Sungkyunkwan University 2066, Seobu-ro, Jangan-gu, Suwon, Gyeonggi, 16419, Korea

[d] SKKU Institute of Energy Science and Technology, Sungkyunkwan University, 2066, Seobu-ro, Jangan-gu, Suwon, Gyeonggi, 16419, Korea

† Equally contributed.

aggregation caused quenching, or undesired red-shifts due to overly extended π-conjugation.[7] Therefore, precise molecular design is highly desirable to simultaneously achieve both narrower and blue-shifted emissions. Indolo[3,2,1-*jk*]carbazole (ICz) has recently garnered significant attention as a highly rigid tripod core, planar building block suitable for constructing narrowband emitters.[8] The seminal report by our group demonstrated a violet-emitting molecule, **tDIDCz**, by fusing two ICz units through *meta*-configured nitrogen atoms, achieving a remarkably narrow FWHM of 14 nm and a CIE*y* of 0.02.[8c] Following this, several modifications of ICz-based systems improved device performance, but often at the cost of red-shifted emissions or spectral broadening.[8d–e] These findings highlight that strategic modifications of the ICz-core can control the emission in the violet and UV range, while ensuring narrowband emission. Carbazole is another key building block widely used in OLED materials, owing to its excellent hole-transport properties, high triplet energy (> 2.8 eV), and versatile functionalization potential. Among its various positions, the C1-site remains relatively underexplored due to synthetic challenges.[9] However, substitution at this position induces significant steric-shielding, causing the appended moiety to adopt a non-planar geometry. This out-of-plane orientation disrupts π-conjugation with the central carbazole, rigidifies the overall molecular structure, and raises the singlet energy, thereby favouring emission in the UV region. While a few NUV emitters based on this approach have been developed, they typically emit > 400 nm with a broad FWHM > 40 nm.[9] By exploiting the aforementioned individual merits of ICz and carbazole, we hypothesize that integrating a rigid ICz unit at the C1-position of carbazole would offer a promising strategy to construct efficient pure UV emitters. The ICz core promotes narrowband emission, while the C1-substitution on carbazole increases the bandgap and singlet energy, effectively pushing the emission into the deep-UV region. This synergistic design holds potential for realizing pure UV emitters with narrow FWHM, addressing long-standing challenges in OLED emitter development.

To authenticate our design strategy, we developed a pure violet emitter by linking the ICz unit at its C5 position to the C1 position of carbazole, resulting in the compound 2-(9-phenyl-9*H*-carbazol-1-yl)indolo[3,2,1-*jk*]carbazole (**1CzICz**) and compared with the reference compound 2-(9-phenyl-9*H*-carbazol-3-yl)indolo[3,2,1-*jk*]carbazole (**3CzICz**). This specific C1-linkage was chosen to promote a rigid molecular geometry, effectively reducing vibronic coupling and enabling a narrow emission with FWHM < 20 nm. Moreover, the spatial separation and steric hindrance between the ICz and carbazole units were expected to suppress interchromophoric interactions, thereby maintaining high singlet and triplet energy. As anticipated, **1CzICz** exhibited a sharp UV emission peak centered at 380 nm with a narrow FWHM of 18 nm compared to the reference compound **3CzICz** ($\lambda_{em} \sim 405$ nm, FWHM ~ 40 nm). The emitter also showed excellent thermal robustness, with a decomposition temperature (T_{5d}) of 376 °C, reflecting the intrinsic rigidity of the ICz and carbazole frameworks. When incorporated into an OLED device, **1CzICz** emitted UV light with an EL peak at 387 nm and a CIE*y* coordinate of 0.037, and delivered a maximum EQE (EQE$_{max}$) of 3.5%. In addition to its

role as an emitter, the high triplet energy and wide bandgap of **1CzICz** rendered it suitable as a host for green phosphorescent OLEDs. Remarkably, the device achieved an EQE$_{max}$ of 22.5% with an ultra-low efficiency roll-off of just 4.0%, while sustaining a high EQE of 21.8% even at a luminance of 3000 cd m^{-2}.

The molecular design in this work focuses on establishing a simple steric-shielding approach for constructing narrowband UV emitters. The ICz core, known for its rigid and planar tripod-like geometry, plays a key role in suppressing vibronic coupling, making it an ideal scaffold for narrowband emissive fluorophores. Moreover, ICz features a deep-lying HOMO level, which is beneficial for engineering wide-bandgap materials. Carbazole, on the other hand, is a widely used building block due to its high E_T, efficient hole-transporting ability, and flexible positional accessibility for substitution. By leveraging the complementary attributes of these two molecular cores, we designed a novel compound by integrating ICz at the sterically hindered C1-position of carbazole, and validated it by comparison with the C3-position (Fig. 1a). Due to the significant steric congestion at the C1-position, the ICz unit is expected to adopt a twisted geometry with respect to the carbazole plane, leading to a non-conjugated molecular architecture. This spatial de-coupling disrupts interchromophoric interactions and effectively increases both the singlet energy and triplet energy, thereby enlarging the optical bandgap and promoting pure UV emission. Simultaneously, the inherent rigidity of the ICz unit suppresses vibronic relaxation, resulting in a narrow emission bandwidth (FWHM < 20 nm) compared to **3CzICz**. The **3CzICz** was synthesized as per the literature procedure.[2e] The synthetic route to the target emitter, **1CzICz**, is outlined in Scheme S1. Intermediate **1** was reacted with 2-(4,4,5,5-tetramethyl-1,3,2-dioxaborolan-2-yl)indolo[3,2,1-*jk*]carbazole using Pd-catalyzed Suzuki–Miyaura cross-coupling to afford the final narrowband UV emitter, **1CzICz**. The structure was confirmed by nuclear magnetic resonance (NMR) spectroscopy and high-resolution mass spectrometry (HRMS). For OLED device fabrication, **1CzICz** was further purified *via* vacuum train sublimation to ensure the high purity necessary for reliable performance.

To gain insight into the molecular geometry, electronic structure, and frontier orbital distribution, HOMO and LUMO of the compounds, we carried out density functional theory
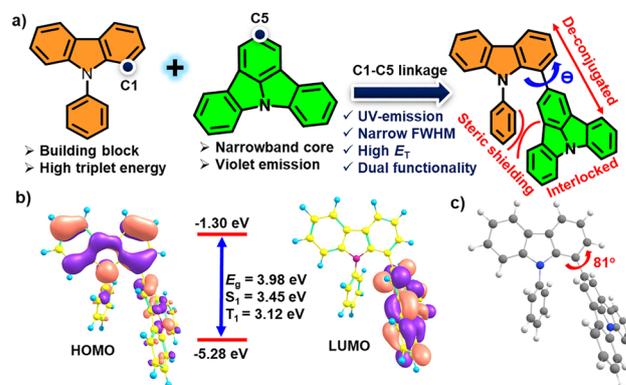

Fig. 1 (a) Strategic molecular design; (b) FMO distribution; (c) optimized geometry.

(DFT) calculations on their fully optimized geometries. The HOMO/LUMO distribution and optimized geometries of the compounds are illustrated in Fig. 1b and Fig. S3. The dihedral angle between ICz and Cz is significantly larger at 81° for the **1CzICz** compared to that of 31° for **3CzICz**, positioning the ICz moiety markedly out of plane relative to the carbazole core. This pronounced torsion effectively disrupts π-conjugation and minimizes interchromophoric interactions between the two fragments in **1CzICz**, leading to an increased singlet excited-state energy and a wider band-gap (E_g). Importantly, this rigid molecular core can suppress the structural alterations in the excited state and narrow the emission FWHM (*vide infra*). This is also evident from the low reorganization energy (λ_s = 0.16 eV) and root mean square displacement (RMSD = 0.18 Å) values between the S_0 and S_1 states of **1CzICz** compared to **3CzICz** (λ_s = 0.20 eV, RMSD = 0.39 Å) (Fig S1 and S2). The HOMO of **1CzICz** is predominantly localized on the carbazole unit with minor delocalization into the ICz moiety, while in **3CzICz** the HOMO is delocalized on both the ICz and Cz units, indicating that effective π-conjugation was limited in the former. The LUMO of the compounds is entirely confined to the ICz fragment. The natural transition orbitals also showed the same trend (Fig. S3). The calculated HOMO/LUMO/E_g for **1CzICz** is −5.28 eV/−1.30 eV/3.97 eV and that for **3CzICz** is −5.11 eV/−1.31 eV/3.80 eV, while the triplet energy is calculated to be high at 3.12 eV for **1CzICz** compared to that of 2.89 eV for **3CzICz**, making it suitable as a host material for other primary color emitters. Based on these computational insights, **1CzICz** is anticipated to exhibit narrowband UV emission with excellent photophysical properties.

The thermal stability of the compounds was assessed using thermogravimetric analysis (TGA) under an inert atmosphere with a heating rate of 10 °C min⁻¹. The TGA curve is shown in Fig. S4, and key data are summarized in Table S1. The compounds exhibited a high thermal decomposition temperature, with a 5% weight loss (T_{5d}) occurring above 350 °C. Specifically, **1CzICz** showed excellent thermal stability with a T_{5d} of approximately 376 °C. The electrochemical properties were investigated *via* cyclic voltammetry (CV) in a dilute dichloromethane solution using tetrabutylammonium perchlorate as the supporting electrolyte and ferrocene as the internal reference (Fig. S5). The compounds exhibited a positively shifted oxidation wave relative to ferrocene, which is attributed to electron removal from the carbazole core. The **3CzICz** displayed a low oxidation onset potential of −0.76 V compared to that of −0.91 V for **1CzICz** due to elongation of the conjugated backbone. Based on these values, the HOMO/LUMO energy levels were estimated using literature-reported methods and calculated to be −5.71/−2.36 eV for **1CzICz** and −5.56/−2.34 eV eV for **3CzICz**. Minor discrepancies between these experimentally obtained energy levels and the DFT-calculated values are likely due to solvation effects and environmental interactions in the experimental setup.

The optical properties of the compounds, such as electronic absorption and emission, were investigated in toluene solution and in DPEPO-doped thin films (Fig. 2 and Fig. S6). The key photophysical parameters are summarized in Table S1. The absorption spectrum of the compounds displayed multiple
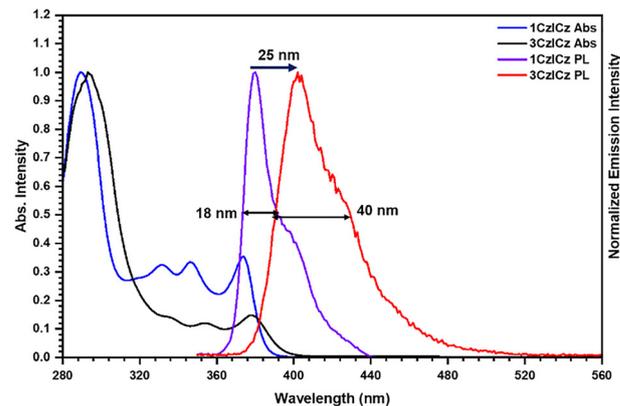

Fig. 2 Photophysical properties of the **1CzICz** recorded in toluene.

bands: the high-energy bands (below ∼350 nm) correspond to localized π–π* transitions within the ICz or carbazole units, whereas the absorption band above 370 nm is attributed to delocalized π–π* transitions involving both the ICz and carbazole fragments. **1CzICz** exhibited 25 nm blue-shifted emission with a sharp UV emission peak at 380 nm compared to **3CzICz**, which is attributed to the interrupted interchromophoric interactions between the ICz and carbazole units. This interpretation is supported by the DFT results discussed earlier. Notably, the **1CzICz** demonstrated ultra-narrowband emission with a FWHM of just 18 nm compared to that of 40 nm for **3CzICz**. This narrow emission is attributed to the high molecular rigidity imparted by the ICz core and the restricted rotation at the C1-substituted carbazole, which suppresses excited-state structural relaxation and minimizes vibronic coupling as evident from its low λ_s and RSMD values. A small Stokes shift of 6 nm further supports the rigidity of the excited-state geometry, indicating minimal structural reorganization upon excitation and suggesting that the emission originates from a locally excited (LE) state. Solvatochromic studies (Fig. S7) further corroborate this conclusion. The emission profiles of the compounds remained unchanged across solvents of varying polarity, from non-polar cyclohexane to polar DMF, indicating that the excited state is non-polar in nature. The absolute photoluminescence quantum yield (PLQY) in solution/film, measured using an integrating sphere, was found to be 89%/42% for **1CzICz** and 72%/38% for **3CzICz**. The low PLQY of the compounds in film form may be due to the concentration quenching. The triplet energies of the compounds were determined from the phosphorescence spectrum recorded at 77 K in frozen THF (Fig. S8). The phosphorescence exhibited structured features similar to the fluorescence spectrum, suggesting emission from a local triplet excited state (^{3}LE). The E_T value, estimated from the onset of the lowest vibronic peak, was 3.05 eV for **1CzICz** and 2.89 eV for **3CzICz**. This is significantly higher than that of the green phosphor, Ir(ppy)$_3$ (E_T ≈ 2.49 eV), ensuring efficient energy transfer while effectively preventing reverse energy transfer from the dopant to the host.

The outstanding photophysical characteristics of **1CzICz**—including its pure UV emission, narrow FWHM, high PLQY, E_T, and superior thermal stability—prompted an exploration of its
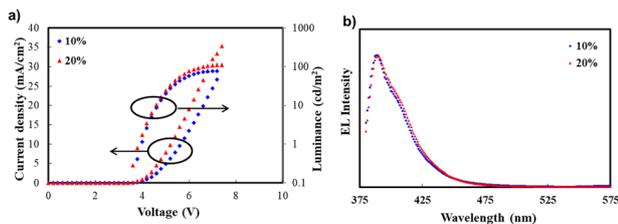
Fig. 3 (a) *I–V–L* and (b) EL spectra of the FOLED of **1CzICz**.

dual role as both an emitter and a host material for green PhOLEDs. The fluorescent OLED device architecture and corresponding energy level alignment are illustrated in Fig. S9. The emitting layer (EML) consisted of **1CzICz** doped at either 10 wt% or 20 wt% in a DPEPO host matrix. Fig. 3 presents the current density–voltage–luminance (*J–V–L*) characteristics and electroluminescence (EL) spectra, with key performance metrics summarized in Table S2. As shown in Fig. 3b, the EL spectrum of the device containing 10 wt% **1CzICz** closely matches its PL spectrum in solution, emitting in the UV region with a λ_{EL} at 387 nm and an FWHM of 28 nm. This spectral alignment confirms that the emission originates from the target EML. Importantly, no noticeable spectral shift was observed upon increasing the doping level to 20 wt%, which can be attributed to the non-planar molecular geometry induced by interlocking of ICz at the C1-position of carbazole, effectively suppressing aggregation-induced emission changes. The device exhibited excellent violet color purity, with CIE coordinates of (0.17, 0.037), owing to its narrow emission bandwidth. Enhancing the doping concentration from 10 wt% to 20 wt% led to improved *J* and *L*, likely due to enhanced dopant-assisted charge injection. As a result, the EQE$_{max}$ increased from 3.1% to 3.5%, with the 20 wt% doped device demonstrating superior overall performance.

In addition to its function as an emitter, **1CzICz** was also evaluated as a host material for green phosphorescent emitters. A PhOLED was fabricated using **1CzICz** as the host and 5 wt% Ir(ppy)$_3$ as the guest dopant. The device structure and energy-level diagram are depicted in Fig. S10, and its *J–V–L* and EQE *vs. L* are shown in Fig. S11. The EL spectrum revealed a sharp green emission peak at 513 nm with CIE coordinates of (0.29, 0.64). The absence of residual emission from the host confirmed efficient energy transfer from **1CzICz** to the guest phosphor. The green PhOLED exhibited a low V_{on} of 5.7 V and delivered excellent device metrics: a maximum EQE of 22.9%, a CE of 79.2 cd A^{-1}, and a PE of 80.6 lm W^{-1}. Remarkably, the device maintained stable EQE at high luminance levels, with an EQE of 22.0% at 3000 cd m^{-2} and a minimal efficiency roll-off of only 4.0%. This outstanding performance is attributed to the efficient exciton confinement and balanced charge transport. These findings underscore the promise of C1-substituted, high-E_T carbazoles as efficient hosts for PhOELDs compared to the conventional hosts mCP and CBP (EQE < 20%).[1d,e]

In conclusion, we have presented a streamlined molecular design for achieving both narrowband and UV emission by integrating a rigid ICz with a carbazole core at a sterically hindered position. The structural design, featuring interlocked geometry and disrupted π-conjugation, led to **1CzICz** exhibiting sharp UV emission centered at 380 nm with an impressively narrow FWHM of just 18 nm compared to **3CzICz**. The **1CzICz** also demonstrated excellent thermal robustness, with a T_{5d} around 376 °C. When implemented in an OLED device as a UV emitter, **1CzICz** achieved an EQE$_{max}$ of 3.5%, accompanied by a violet CIEy coordinate of 0.037. Furthermore, its high triplet energy and wide bandgap made it a suitable host material for green PhOLEDs. In this role, the device delivered outstanding performance, including an EQE$_{max}$ of 22.9%, a CE of 79.2 cd A^{-1}, and an exceptionally low efficiency roll-off of 4.0% at a luminance of 3000 cd m^{-2}. Overall, these results highlight the potential of the steric-shielding strategy in designing high-efficiency, narrowband B-free UV emitters with multifunctional applicability for OLEDs.

Conflicts of interest

There is no conflict to declare.

Data availability

The data supporting this article have been included as part of the supplementary information (SI). Supplementary information: experimental methods, NMR, photophysical, TGA and OLED data. See DOI: **https://doi.org/10.1039/d5cc04554a**.

References

1 (*a*) Y. Kondo, *et al.*, *Nat. Photonics*, 2019, **13**, 678; (*b*) P. Keerthika, *et al.*, *Adv. Opt. Mater.*, 2023, **11**, 2301732; (*c*) X. Wu, *et al.*, *Chem. Rev.*, 2025, **125**, 6685; (*d*) R. Braveenth, *et al.*, *Dyes Pigm.*, 2019, **162**, 466; (*e*) H. Huang, *et al.*, *Chem. – Eur. J.*, 2013, **19**, 1828.

2 (*a*) X. Wang, *et al.*, *Chem. Sci.*, 2025, **16**, 7495; (*b*) J. M. Ha, *et al.*, *NPG Asia Mater.*, 2021, **13**, 53; (*c*) X. He, *et al.*, *Angew. Chem., Int. Ed.*, 2022, **61**, e20229425; (*d*) Y. Xiao, *et al.*, *Chem. Sci.*, 2022, **13**, 8906; (*e*) J. Hong, *et al.*, *Synth. Mater.*, 2025, **311**, 117845.

3 (*a*) Y. Kitamoto, *et al.*, *Angew. Chem., Int. Ed.*, 2025, **64**, e202510891; (*b*) H. Qi, *et al.*, *ACS Mater. Lett.*, 2025, **7**, 1019; (*c*) F. Zhan, *et al.*, *Angew. Chem., Int. Ed.*, 2025, **64**, e202505328; (*d*) J. Chen, *et al.*, *Angew. Chem., Int. Ed.*, 2022, **61**, e202116810; (*e*) P. Kaunty, *et al.*, *Org. Electron.*, 2016, **34**, 237; (*f*) S. Zou, *et al.*, *Adv. Opt. Mater.*, 2020, **8**, 2001074; (*g*) H. Zhang, *et al.*, *Angew. Chem., Int. Ed.*, 2021, **60**, 22241.

4 (*a*) H. Uoyama, *et al.*, *Nature*, 2012, **492**, 234; (*b*) Z. Yang, *et al.*, *Chem. Soc. Rev.*, 2017, **46**, 915; (*c*) X. Geo, *et al.*, *Small*, 2022, **18**, 2204029; (*d*) M. A. E. Ain, *et al.*, *J. Mater. Chem. C*, 2025, **13**, 12504; (*e*) Y. Luo, *et al.*, *Adv. Mater.*, 2020, **32**, 2001248; (*f*) F. Hu, *et al.*, *Chem. Eng. J.*, 2023, **464**, 142678; (*g*) Y. Xiao, *et al.*, *Chem. Sci.*, 2022, **13**, 8906.

5 (*a*) X. F. Luo, *et al.*, *Chem. Commun.*, 2024, **60**, 1089; (*b*) R. K. Konidena, *et al.*, *Adv. Photon. Res.*, 2022, **3**, 2200201.

6 (*a*) G. Li, *et al.*, *J. Am. Chem. Soc.*, 2024, **146**, 1667; (*b*) X. Gan, *et al.*, *Adv. Opt. Mater.*, 2023, **11**, 2300195; (*c*) H. J. Kim, *et al.*, *Adv. Funct. Mater.*, 2021, **31**, 2102588; (*d*) J. Park, *et al.*, *Adv. Opt. Mater.*, 2024, **12**, 2302791.

7 (*a*) H. Qi, *et al.*, *Chem. Sci.*, 2024, **15**, 11053; (*b*) L. Peng, *et al.*, *Chem. Eng. J.*, 2022, **450**, 138339.

8 (*a*) X. Wang, *et al.*, *Chem. – Eur. J.*, 2023, **29**, e202300701; (*b*) H. L. Lee, *et al.*, *Small*, 2020, **16**, 1907569; (*c*) J. A. Seo, *et al.*, *ACS Appl. Mater. Interfaces*, 2017, **9**, 37864; (*d*) R. K. Konidena, *et al.*, *J. Org. Chem.*, 2022, **87**, 6668; (*e*) J. Wei, *et al.*, *Angew. Chem., Int. Ed.*, 2021, **60**, 12269.

9 (*a*) H. Huang, *et al.*, *Chem. – Eur. J.*, 2013, **19**, 1828; (*b*) R. K. Konidena, *et al.*, *J. Ind. Chem. Eng.*, 2022, **107**, 75; (*c*) T. Yang, *et al.*, *J. Phys. Chem. C*, 2024, **128**, 16085.